North American Droughts in ERA-40 Global and NCEP North American Regional Reanalyses: A Palmer Drought Severity Index Perspective

KRISTOPHER B. KARNAUSKAS, ALFREDO RUIZ-BARRADAS, SUMANT NIGAM, AND ANTONIO J. BUSALACCHI

Department of Atmospheric and Oceanic Science, and Earth System Science Interdisciplinary Center, University of Maryland, College Park, College Park, Maryland

(Manuscript received 2 January 2007, in final form 10 August 2007)

ABSTRACT

The Palmer drought severity index (PDSI) monitors meteorological and surface hydrological parameters to represent the severity of drought conditions. PDSI datasets are developed for the NCEP North American Regional Reanalysis (NARR) and the 40-yr European Centre for Medium-Range Weather Forecasts (ECMWF) Re-Analysis (ERA-40) to facilitate North American drought research with these datasets. The drought index calculation, in particular, allows diagnostic assessment of the relative contributions of various surface water balance terms in generation of drought conditions by selectively holding these terms to their climatological value in PDSI computations. The length of the diagnosed PDSI permits analysis of subdecadal time-scale variability, such as ENSO, whose influence on North American drought evolution is investigated. ENSO's considerable drought impact is potentially predictable, especially in the southern half of the United States.

1. Introduction

Estimates of annual economic loss in the United States directly attributable to drought are in the range of $6–8 billion. In response to growing concern from local and national leadership, the National Integrated Drought Information System (NIDIS) has been established to synthesize the work of modeling and reanalysis communities with that of monitoring and application communities. The most widely used index to monitor drought conditions in the United States is the Palmer drought severity index (PDSI). The PDSI algorithm was originally devised by Palmer (1965) as an index to monitor long-term or cumulative meteorological drought conditions from precipitation, surface air temperature, and available water content. Each component of the water balance, including evaporation, soil recharge, runoff, and loss (penetration of moisture through the surface layer) are accounted for. The PDSI takes a supply-and-demand approach to the surface water balance, and the treatment of moisture conditions as measurements standardized by regional characteristics allows for meaningful spatial and temporal comparisons.

In response to an array of assessments of the PDSI (e.g., Alley 1984; Karl 1986), the National Oceanic and Atmospheric Administration/Climate Prediction Center (NOAA/CPC) and others have devised new indices as complements to the PDSI. Some of these include a crop moisture index, a topsoil moisture index, and objective short- and long-term drought indicator blends. The short- and long-term drought indicator blends are meant to separate the drought conditions into effects that respond to short-term variability from those that respond to longer-term cumulative variability. These indices synthesize existing indices and the NOAA/CPC soil moisture model. There are numerous other useful means of defining drought, such as the standardized precipitation index (SPI), modeled soil moisture anomalies, and streamflow. Even in light of the growing number of alternatives, the PDSI remains the most popular drought index in the United States (Heim 2002). For research purposes, the PDSI is particularly well suited as it accounts for a relatively complete picture of the terrestrial water balance, rather than statistical properties of precipitation or soil moisture alone.

Corresponding author address: Kristopher B. Karnauskas, Lamont-Doherty Earth Observatory, Columbia University, 301F Oceanography Building, 61 Route 9W, Palisades, NY 10964.
E-mail: krisk@ldeocolumbia.edu

DOI: 10.1175/2007JCLI1837.1

While North American droughts are often characterized using the observation-based PDSI index, investigations of drought genesis and maintenance typically involves analysis of related atmospheric circulation anomalies. Modern retrospective analyses (i.e., reanalyses) such as the global 40-yr European Centre for Medium-Range Weather Forecasts (ECMWF) Re-Analysis (ERA-40; Uppala et al. 2005) and the regional National Centers for Environmental Prediction (NCEP) North American Regional Reanalysis (NARR; Mesinger et al. 2004) datasets have provided valuable multidecade-long circulation datasets for this purpose, but the related hydroclimate in these datasets is not always realistic, especially in ERA-40 where precipitation observations are not assimilated. The lack of full consistency between the observation-based PDSI and the reanalysis circulation and hydroclimate has not been helpful, and the present study offers a partial solution by diagnosing PDSI directly from the ERA-40 and NARR hydroclimate fields.

A growing body of research has been aimed at understanding the relationships between precipitation and specific modes of interannual and decadal climate variability. In particular, the relationship between rainfall anomalies in the U.S. Great Plains region and sea surface temperature variability has recently come into focus. The important role of El Niño–Southern Oscillation (ENSO) has been established by recent observational and modeling studies (e.g., Trenberth and Guillemot 1996; Mo et al. 1997; Dai et al. 1998; Barlow et al. 2001; Schubert et al. 2004). The common thread is that ENSO is the fundamental driver of global drought patterns, and La Niña events play a particularly important role in the initiation of atmospheric circulation anomalies in the midlatitudes that leads to North American drought.

Nigam et al. (1999) directly addressed the linkages between U.S. drought and Pacific decadal variability using the PDSI. Barlow et al. (2001) expounded upon the results of Nigam et al. (1999), establishing mechanistic links for the ENSO and Pacific decadal variability influence. The linkages with Great Plains precipitation anomalies were further corroborated by the model-based investigation of Schubert et al. (2004), although not with PDSI calculations. Given that drought conditions rely heavily upon cumulative hydrological processes including precipitation and temperature, linkages between PDSI and large-scale climate variability should be investigated with respect to recognized modes of variability in the tropics and Northern Hemisphere.

An overview of the PDSI algorithm, the reanalyses and external data used to construct new PDSI datasets, and unique aspects of our methodology are provided in the following section. The major results are presented and discussed in section 3, and a summary of the major findings, along with potential implications, is provided in section 4.

2. Data and methods

In its most primitive form, the PDSI is an algorithm that requires little more than precipitation and temperature to infer a great deal of information about the state of the surface hydrological budget and how the soil responds on a local basis. Dai et al. (2004) produced a monthly, global (2.5° by 2.5° horizontal resolution) PDSI dataset over global land areas for the period 1870–2003 using exclusively in situ temperature and precipitation data. The Climate Research Unit (CRU) surface air temperature (Jones and Moberg 2003) and NOAA/CPC precipitation (Chen et al. 2002) were the observational datasets chosen by Dai et al. The PDSI study of Dai et al. was one from which variability on long time scales may be assessed. However, use of regional and global reanalyses allows one to take advantage of explicitly provided hydrological variables (e.g., potential evaporation or soil moisture in multiple layers) that link the regional terrestrial and atmospheric water cycles.

The crux of the PDSI is the difference between the actual precipitation (P) and the amount of precipitation required to maintain a climatologically appropriate soil moisture level for the month (P_{req}). This difference can be written as $d = P - P_{\text{req}}$. Thus, for a month during which more precipitation fell than was required to maintain normal soil moisture, d would be positive and wet conditions prevail. The real challenge to PDSI is determining P_{req}. The P_{req} is subject to the requirements of the water balance $P_{\text{req}} = \alpha\text{PE} + \beta\text{PR} + \gamma\text{PRO} + \delta\text{PL}$, where PE is potential evaporation, PR is potential recharge, PRO is potential runoff, and PL is potential loss. The coefficients α, β, γ, and δ represent the expected ratios of actual-to-potential evaporation, recharge, runoff, and loss, respectively. Thus, αPE is proportional to actual evaporation, and so on.[1] Available water content (AWC) is relevant in the potential fields (e.g., the more AWC, the greater potential for evaporation), and temperature is relevant in the ex-

[1] The surface water balance may be written $\partial S/\partial t = P - E - \text{RO} - L$ (where S is soil moisture). If we express the left-hand side as $S_c - S_o$, where subscripts c and o are climatological and observed values, $\partial(S_c - S_o)/\partial t$ will be the potential recharge (PR). Rearranging yields the stated equation $P = E + R + \text{RO} + L$.

pected ratios (e.g., the higher the temperature, the more evaporation expected). The AWC used in the present study, as in that of Dai et al. (2004), is based on Webb et al. (1993), which derived water-holding capacity based on soil texture. An alternative method of deriving PDSI from the NARR without using external AWC data is given by Mo and Chelliah (2006); the authors became aware of this paper at revision time. Finally, d is weighted by K, an empirical coefficient that depends on the local climate and calendar month. The local climate coefficient K, as well as many other parameters, are necessarily dependent on temporal period of the available input data. Thus, droughts and wet spells will effectively relate to what is "normal," averaged over the period of the reanalyses (discussed in the following paragraph), and not take into account long-term trends in, for example, temperature and precipitation. The expression for the monthly Z value is thus $Z = Kd$. In order that the PDSI does not change rapidly from month to month in response to transient weather events, the PDSI is a weighted sum of the contemporaneous Z value and antecedent PDSI. The PDSI–Z relationship can be expressed as $\mathrm{PDSI}_t = A\mathrm{PDSI}_{t-1} + BZ_t$, where A and B were empirically determined by Palmer (1965) to be 0.897 and 0.333, respectively. PDSI values typically range from −4 to +4, where negative values signify dry conditions and positive values signify wet conditions.

In this study, we have chosen to adapt the PDSI algorithm to NARR and ERA-40. The NARR is the only regional reanalysis of its kind for North America and directly assimilates observations including precipitation. One limitation of the NARR is that assimilation of precipitation over Canada is sparse compared to that over the United States, which may have an impact on our results as we calculate PDSI over the broader North American domain [for an overview of observational data assimilated into the NARR see Shafran et al. (2005)]. The basis of the NARR is the Eta regional atmospheric model (Black 1994), the Noah comprehensive land surface model (Ek et al. 2003), and the assimilation of satellite radiances and high-quality precipitation observations, for which the NARR is unique. The spatial resolution of the NARR is 32 km by 45 levels in the vertical; however, we use a uniform 1° by 1° grid. Lateral boundary conditions for the regional reanalysis are provided by the NCEP–National Center for Atmospheric Research (NCAR) global reanalysis (Kalnay et al. 1996). The NARR is presently available for the 25-yr period January 1979–December 2003. In addition to the usual atmospheric fields, the NARR is thought to be especially well suited for describing the land surface state and fluxes of water and energy (Nigam and Ruiz-Barradas 2006).

While the ERA-40 does not directly assimilate precipitation, it does benefit from improvements in data assimilation over the past decade (e.g., assimilation of radiances from NOAA polar-orbiting satellites). The ERA-40 is preferred over the NCEP–NCAR reanalysis due to the relatively poor representation of North American precipitation in the NCEP–NCAR reanalysis. On the annual mean, the NCEP–NCAR reanalysis places far too much precipitation over the eastern United States, particularly during boreal summer, and a much exaggerated annual harmonic of precipitation (Nigam and Ruiz-Barradas 2006). ERA-40 shows good correspondence with observations in these aspects of North American hydroclimate. The spatial resolution of ERA-40 is 125 km by 60 levels in the vertical. The horizontal resolutions of the resulting PDSI datasets match those of the gridded reanalyses (1° by 1° for NARR; 2.5° by 2.5° for ERA-40). The algorithms were implemented for the North America region (12°–65°N, 130°–63°W) for the 24-yr period January 1979–December 2002.

The primary objective of Dai et al. (2004) was to compute the PDSI using data traditionally fed into the PDSI algorithm: observed T and P. The goal of the present study is similar except that we take advantage of all relevant reanalysis data, including some intermediate parameters that would otherwise be determined only from relatively crude calculations beginning with T and P. In this manner, we exploit the unique strengths of the reanalyses themselves in representing PDSI conditions. In some respects, this approach renders the task less complicated because both NARR and ERA-40 provide more information about the surface water balance than are available as consistent and reliable observations.

The main complication introduced by our strategy, however, is in dealing with the fact that some parameters are included in one reanalysis but not the other. Relevant parameters provided by *both* the NARR and ERA-40 are surface air temperature, precipitation, evaporation, runoff, and soil moisture. In addition, NARR provides potential evaporation (PE). As in Dai et al. (2004) and Palmer (1965), the Thornwaite (1948) method was used to calculate PE for ERA-40. The mainly empirical PE method of Thornwaite (1948) has some known problems, including underestimation of PE in arid regions, while it has been shown to produce reasonably accurate results for large enough areas (Palmer and Havens 1958). Other methods such as Penman (1948) and Budyko (1958) have been proposed (for a comparison see Sellers 1964). However, the

Thornwaite remains the simplest and most widely used method of estimating PE, and allows us to compare results with Dai et al. (2004) with fewer inherent inconsistencies. Other major differences include surface and subsurface runoff in NARR versus total runoff in ERA-40 and different partitioning of soil layers for moisture content between the NARR and ERA-40. The PDSI algorithm does not require runoff at separate layers; thus NARR surface and subsurface runoff are summed to form total runoff. PDSI does, however, require that moisture content be accounted for at two soil layers. The NARR's native soil layers are 0–0.1, 0.1–0.4, 0.4–1.0, and 1.0–2.0 m, while in ERA-40 they are 0–0.07, 0.07–0.28, 0.28–1.0, and 1.0–2.89 m. Thus, the native soil layers in the NARR and ERA-40 do not match except that the third layer in each reanalysis ends at 1 m. Although this is undoubtedly a deeper surface layer envisioned by Palmer (1965), we chose to integrate the top three reanalysis layers to form the PDSI surface layer and use the remaining reanalysis layer (constituting soil below 1 m) to represent the PDSI subsurface layer. This choice allows for even comparisons between NARR and ERA-40 PDSI results with fewer built-in inconsistencies. Initial sensitivity tests have shown that this choice makes little difference in our PDSI results because soil moisture plays a somewhat reduced role in our implementation of the PDSI algorithm; the reason being many hydroclimate parameters such as evaporation, which in nature depend on how much water is present in the surface layer, are provided directly from reanalysis instead of being calculated inside the PDSI algorithm. Only water in liquid form is included in the soil moisture content.

Given the relatively large amount of useful information about the surface water balance provided by the NARR, a diagnostic analysis of the impact of key surface hydrological processes using the NARR is also possible. A simple sensitivity approach was taken by developing modified versions of the NARR PDSI code wherein one component of the surface water balance was held to climatology. These variables included evaporation, potential evaporation, runoff, and soil moisture content. Surface air temperature was not included in the sensitivity analysis because it is only used by the PDSI to calculate evaporation, which is directly provided by the NARR. By subtracting the experimental results (i.e., those generated with one input held to climatology) from the control results (i.e., those generated with all inputs interannually varying), we can isolate the contribution of the variability of a particular hydrological process to that of overall drought conditions.

3. Results

a. Spatial and temporal behavior

Before analyzing the time-dependent characteristics of drought conditions over North America from the newly constructed PDSI datasets, we first examine the basic scales and spatial distribution of PDSI variability. Differences in the amplitude distribution of variability between PDSI and precipitation variability will likely highlight regions whose meteorological drought conditions may be more or less sensitive to precipitation versus other components of the water balance. A simple measure of the range of interannual variability is the standard deviation of monthly anomalies, which is shown for both precipitation and PDSI fields in Fig. 1; distributions from the NARR, ERA-40, and Dai et al. (2004) are intercompared over North America. The monthly PDSI from NARR exhibits relatively high variability over broad regions including the northwest United States, the eastern sector of the Great Plains, and the Southeast. There is a pronounced lack of interannual variability in a band stretching from Mexico to the Canadian border between about 105° and 100°W, with the exception of a localized maximum over northeastern New Mexico and eastern Colorado. Precipitation variability in NARR is also large in the Pacific Northwest but the relative maximum is confined to the Pacific coast; leading to noncollocation of the PDSI and precipitation maxima in the region. In contrast, the maximum in precipitation variability in the Southeast closely matches the position of the counterpart feature in the PDSI field.

The spatial distribution of ERA-40 precipitation variability is similar to that of NARR, including relative maxima along the Pacific Northwest coast and the southeastern United States; but the amplitude is smaller. As in the NARR results, the broad PDSI variability maximum in the Pacific Northwest corresponds to a region of relatively low precipitation variability. Key differences between the NARR and ERA-40 PDSI standard deviations are in the Southeast (NARR has a local maximum while ERA-40 has a minimum) and Mexico (NARR has a minimum while ERA-40 has a maximum). Also, the aforementioned band of minimum PDSI variability evident in the NARR results appears to be missing in ERA-40; however, this is likely due to ERA-40's coarser horizontal resolution. In spite of resolution differences, the overall scale of PDSI variability in NARR and ERA-40 is in good agreement.

It is interesting to compare the PDSI variability in the Dai et al. diagnosis with that of our fields, especially

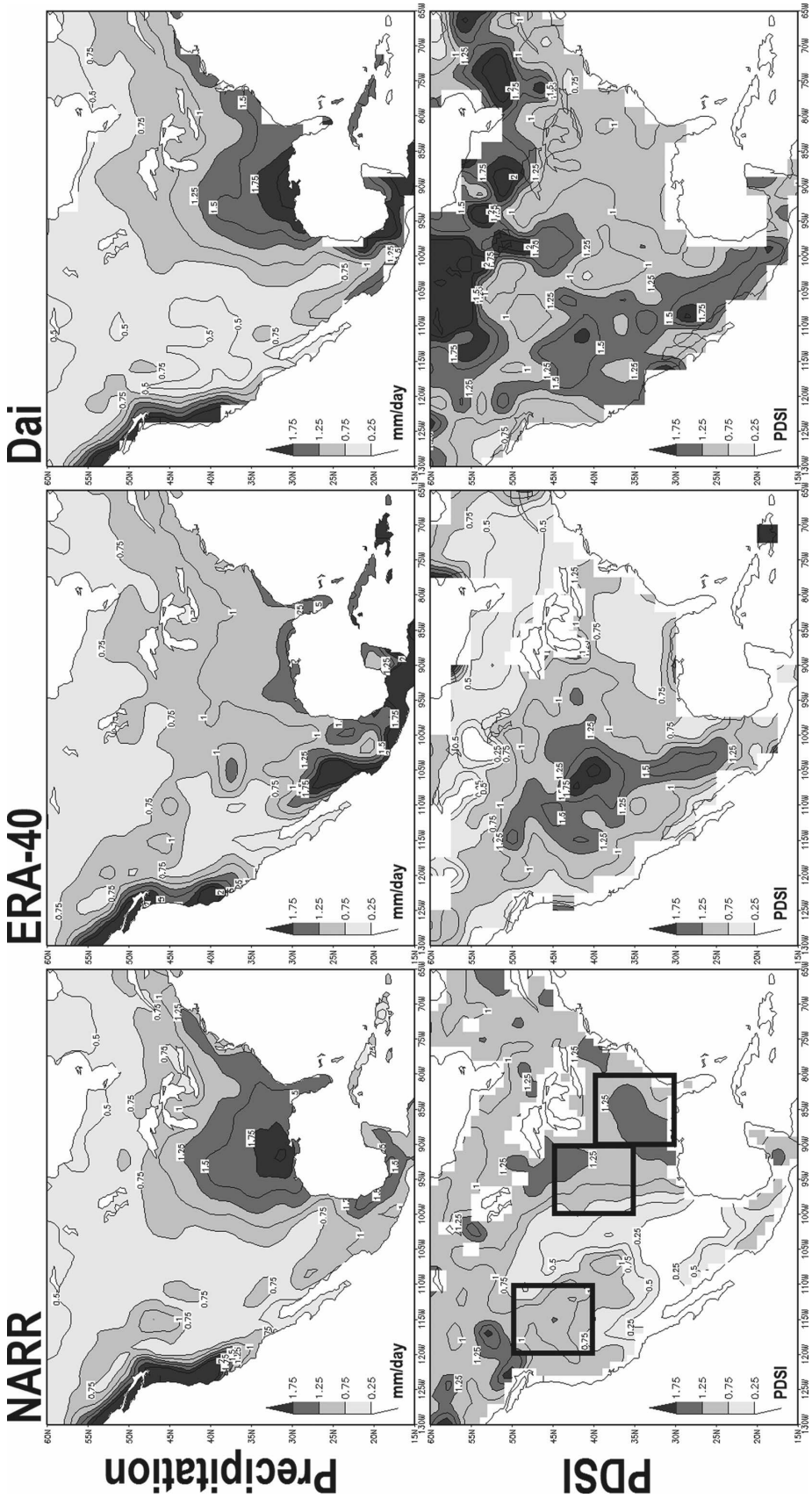

FIG. 1. (top) Standard deviation of monthly precipitation anomalies (mm day^{-1}) and (bottom) the resulting PDSI datasets used in the (left) NARR, (middle) ERA-40, and (right) Dai et al. PDSI calculations over the period from January 1979 to December 2001. A nine-point spatial smoothing was applied to the NARR standard deviation plots. Boxes in the bottom-left panel denote regions used for the area-averaged PDSI indices discussed in the main text and displayed in Fig. 2.

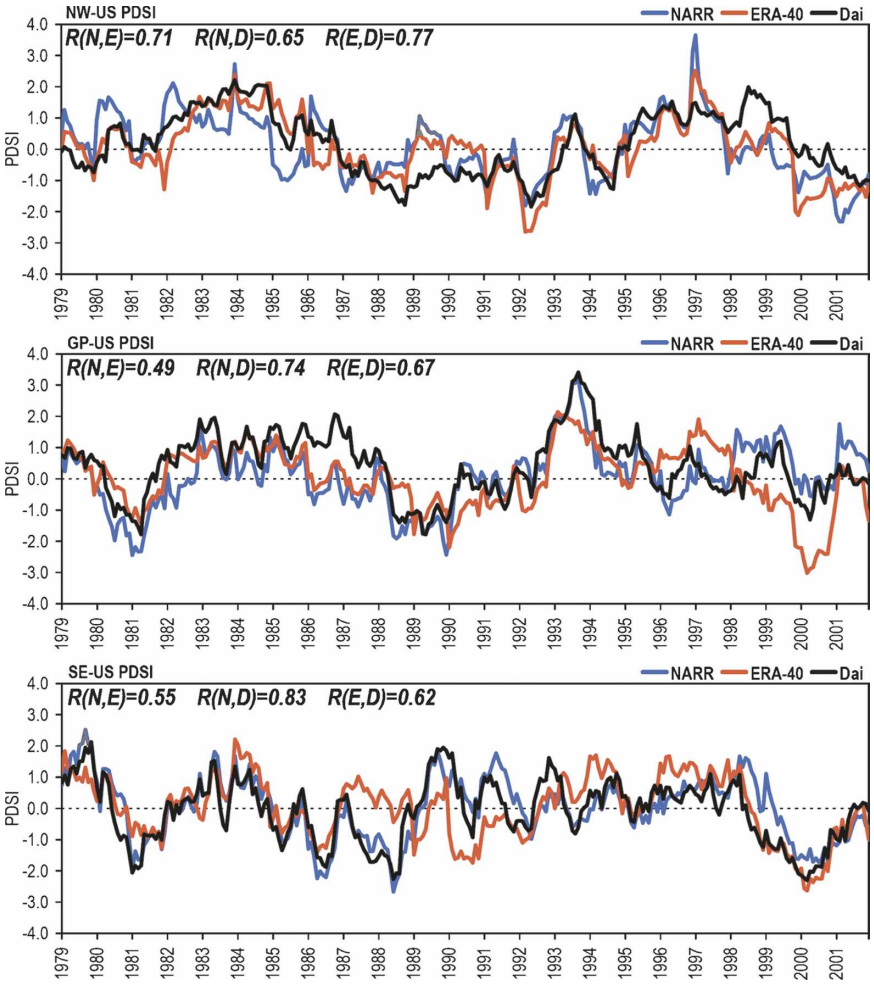

FIG. 2. Normalized (divided by one standard deviation) time series of monthly PDSI indices from NARR (blue), ERA-40 (red), and Dai et al. (2004) (black) for the (top) NW, (middle) GP, and (bottom) SE U.S. regions.

NARR given that these two diagnoses are driven by rather similar precipitation fields.[2] Despite this basis for similarity, Dai's PDSI variability amplitude is closer to ERA-40's than NARR's, attesting to the potential importance of surface air temperature in PDSI diagnosis. Both Dai et al. and ERA-40 exhibit maxima over Mexico and minima over the southeastern United States—the opposite of that seen in the NARR-based diagnosis!

Based on the above examination of the variability range in the newly constructed PDSI datasets and the results of Dai et al., three 10° latitude by 10° longitude regions were chosen (Fig. 1, bottom left) from which area-averaged PDSI indices were constructed. The time-dependent drought characteristics of these indices are examined in this and following sections. Time series of each PDSI index from NARR, ERA-40, and Dai et al. are presented in Fig. 2. The correspondence on interannual and longer time scales of each index between the three datasets is remarkable given the diversity of the precipitation sources (direct assimilation of plentiful observations, calculation plus assimilation of satellite radiances, and coarse observations for NARR, ERA-40, and Dai et al., respectively). Also evident are cyclic patterns of alternating wet and dry subdecadal periods. These are especially distinguishable in the Northwest (NW) and Great Plains (GP) regions (e.g., early 1980s wet, late 1980s and early 1990s dry, mid-1990s wet, etc.). The linear correlation coefficients be-

[2] NARR assimilates observed precipitation quite successfully (e.g., Ruiz-Barradas and Nigam 2006). The NARR precipitation is thus very close to the observed distribution, which is an important driver in the Dai et al. PDSI diagnosis.

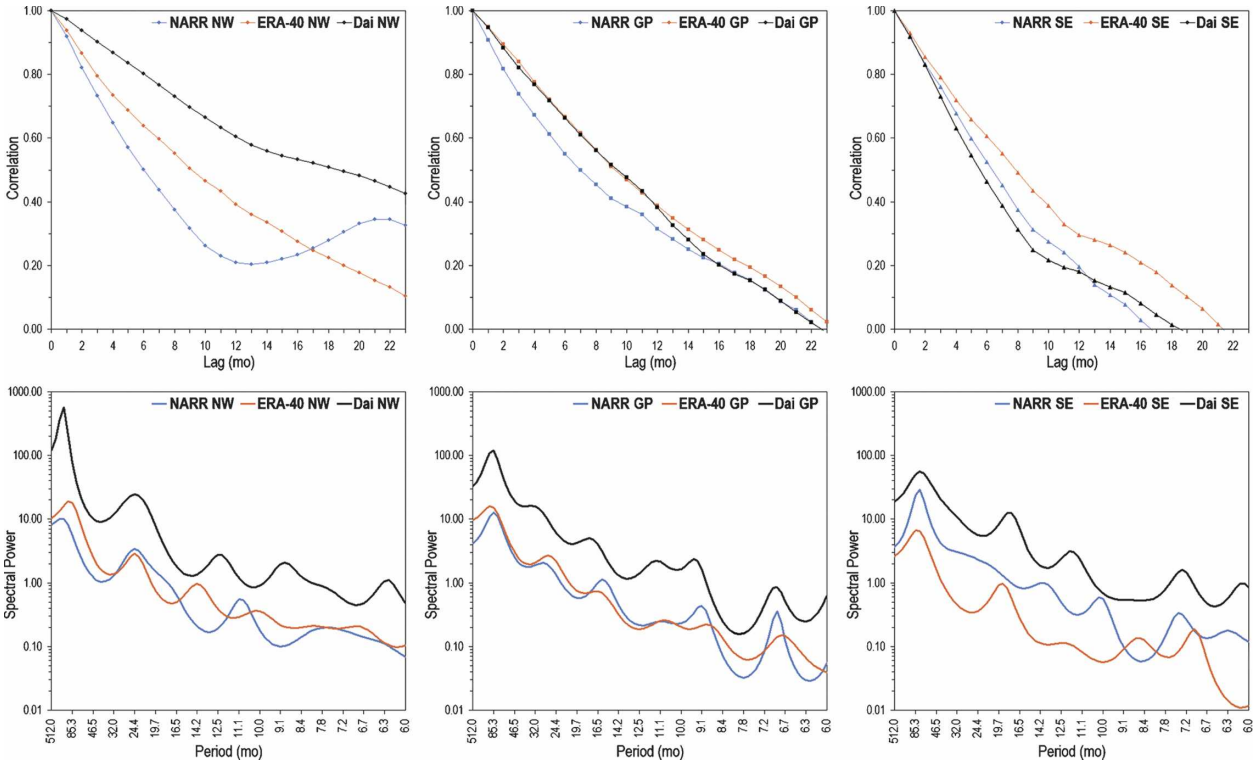

FIG. 3. (top) Autocorrelations and (bottom) power spectra of monthly PDSI indices from NARR (blue), ERA-40 (red), and Dai et al. (2004) (black) for the (left) NW, (middle) GP, and (right) SE regions for the period from January 1979 to December 2001.

tween each dataset for each index are provided in the title line of each time series. Correlations range from 0.55 to 0.83 and all are significant at the 99.5% confidence level, based on a two-tailed Student's *t* test. The two largest discrepancies among all of the regional PDSI indices (Fig. 2) are the ERA-40 overestimation of GP drought conditions in 2000 and nonrepresentation of drought conditions over the Southeast (SE) in 1987–88 (and GP in 1988).

The autocorrelations and power spectra of each PDSI index from each dataset are provided in Fig. 3. Power spectra were produced using the maximum entropy method (MEM; see Ghil et al. 2002). Immediately apparent is the disparity of the autocorrelation functions in the NW region. Similar to the GP and SE autocorrelations, NARR PDSI is less persistent than ERA-40 in the NW region, but the Dai et al. PDSI has a much longer decorrelation time scale than either NARR or ERA-40. For the results from all three datasets, the SE PDSI index decorrelates most rapidly, followed by GP, and the NW. The fact that the Dai et al. NW PDSI index decorrelates the slowest, and that decorrelation time scales decrease eastward across the United States is also evident in the spectral analysis. The spectral power at the lowest frequency peak in Dai et al. (period 128 months) is more than an order of magnitude greater that of ERA-40 (NARR) in the NW region. Interestingly, the period of the first peak at each index is agreed upon by the three datasets except for the NW region. In the NW power spectra, Dai et al. and NARR PDSI have their first peaks at a period of 128 months, whereas the ERA-40 first peak is slightly shorter at 102 months. In either case, the first and strongest peak can be considered a manifestation of the low-frequency cycle evident in the NW time series. With respect to the GP and SE regions, however, the low-frequency peak is not quite decadal; the period of the first peak decreases eastward across the U.S. indices from 102 to 128 months at NW, 85 months at GP, and 73 months at SE. The second spectral peak in all datasets at all indices is found at approximately 20 months, with that number also decreasing from west to east. Finally, we note that the Dai et al. spectra yield higher spectral power at all frequencies and for all indices. This is consistent with the Dai et al. PDSI standard deviation being overall higher than that of NARR and ERA-40.

Dai et al. (2004) identified two leading modes of global PDSI variability throughout the twentieth century: a trend pattern associated with increasing global

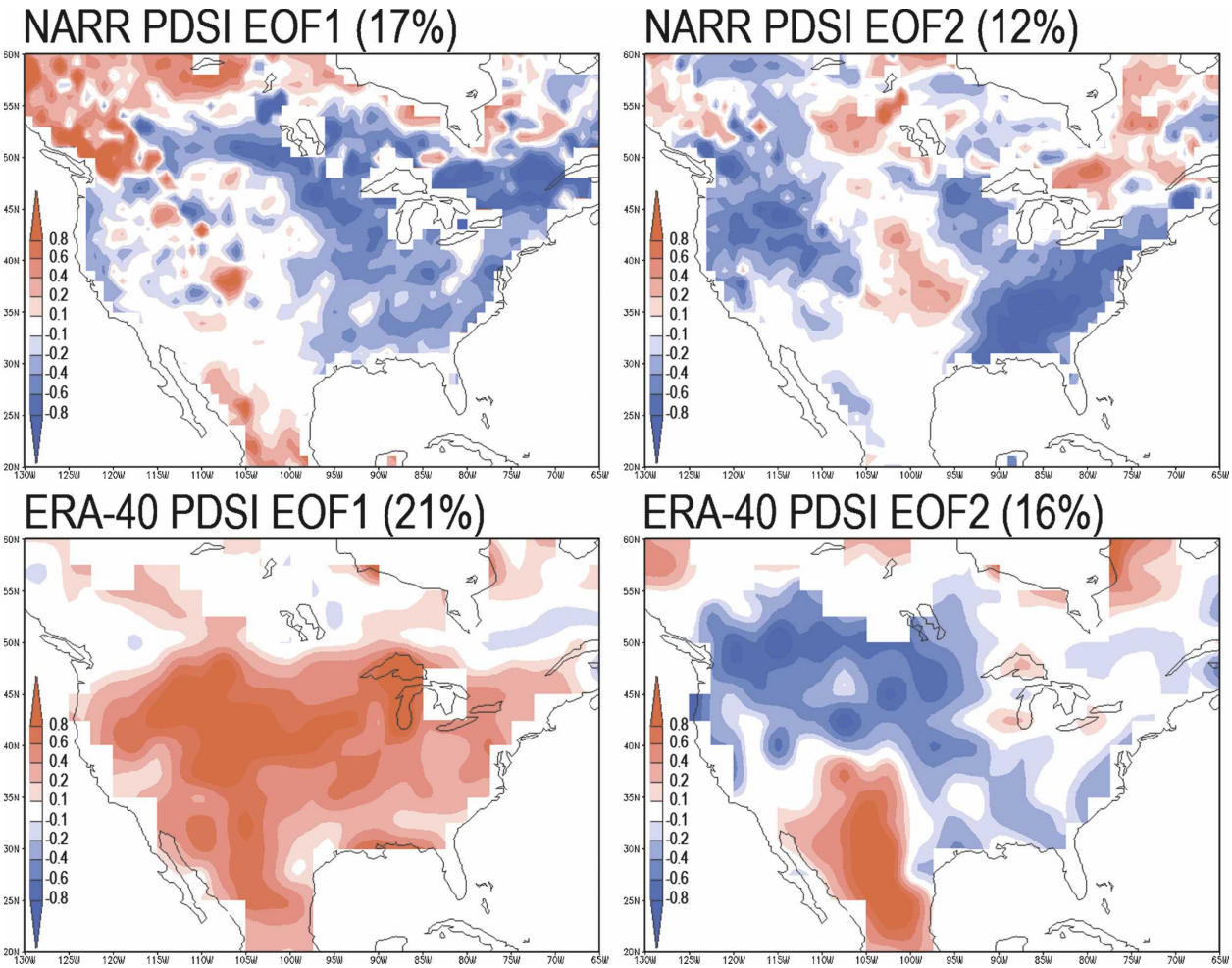

FIG. 4. Leading two EOFs of monthly PDSI from (top) NARR and (bottom) ERA-40 for the period from January 1979 to December 2001 and the spatial domain 20°–60°N, 130°–65°W. The EOFs are scaled by the rms of the corresponding principal components (PCs).

precipitation and modulated by the drying effect of regional patterns of surface warming and a second pattern associated with ENSO. The maximum correlation between ENSO and PDSI was found with ENSO leading PDSI by 6 months. Remotely forced precipitation patterns were inferred to be primarily responsible for the correlation. To characterize the dominant patterns of interannual drought variability over North America, empirical orthogonal function (EOF) analysis was performed on the newly constructed PDSI datasets from NARR and ERA-40. The temporal period and spatial domain used for the hEOF analysis was identical for both NARR and ERA-40 results: from January 1979 through December 2001 over 20°–60°N, 130°–65°W. The first two EOFs are shown in Fig. 4. The leading EOFs (whose PCs explain roughly 20% of the variance in each dataset) are similar in that there is one broad polarity present in the United States. Particularly from the coarser ERA-40, EOF1 describes the United States being in a general state of either drought or wet-spell conditions. This statement is true of the finer NARR PDSI, albeit a lack of loading in the previously described band stretching from Mexico to Canada between about 105° and 100°W (where it happens to be strongest in ERA-40 results). In spite of considerable differences in the spatial patterns in EOF2 between PDSI datasets derived from the NARR and ERA-40, there is good correspondence between principal components (PCs). The PCs (Fig. 5) also hint at variability on time scales ranging from interannual to decadal. The first and second modes extracted from NARR and ERA-40 PDSI are reversed; the first PC from the NARR corresponds with the second PC from ERA-40 (r = 0.72, 99.5% significance) and the first PC from ERA-40 corresponds with the second PC from the NARR (r = 0.70, 99.5% significance). The time- and

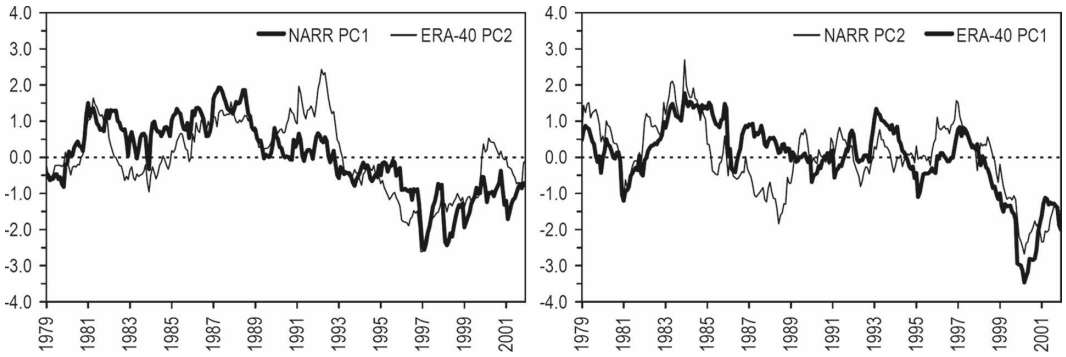

FIG. 5. (left) The first PC of NARR PDSI matched with the second PC of the ERA-40 PDSI and (right) the second PC of NARR PDSI matched with the first PC of ERA-40 PDSI for the period from January 1979 to December 2001 and the spatial domain 20°–60°N, 130°–65°W.

process-dependent evolution of these patterns and indices are discussed in sections 3b–d.

b. PDSI or soil moisture anomaly?

Drought is clearly a difficult phenomenon to define, both in terms of impacts and measurable quantities. Due to the availability and improvements of land surface models and data assimilation, it is becoming increasingly popular to define drought in terms of soil moisture anomalies (e.g., Fan et al. 2006). The purpose of this brief section is to compare and contrast the overall picture of drought depending on whether one considers PDSI or simulated soil moisture anomalies. For this exercise, we will consider the GP region and use the PDSI and soil moisture from the NARR. Just as the area-average PDSI within the GP region was used to construct the GP PDSI time series, the area-average monthly soil moisture anomaly (surface layer, or top 1 m of soil) was computed to generate a GP soil moisture anomaly time series. Next, we choose as criteria for objectively identifying "droughts" ("wet spells") as any instance where the time series is negative (positive) by at least one standard deviation for three or more consecutive months. Applying the above simple algorithm to the GP PDSI and soil moisture anomaly time series yields the depiction shown in Fig. 6. Using the PDSI, two droughts were identified between 1979 and 2001, compared with six identified using the soil moisture anomaly time series.

The important message from the comparison in Fig. 6 is that the soil moisture index is not complete enough to distinguish that a single wet month in terms of surface soil moisture does not necessarily herald the end of a drought. This is especially evident in the severe U.S. drought of 1988. The PDSI index responds appropriately to the two spikes in surface soil moisture in late 1988 and mid-1989, but is not tempted above the −1 standard deviation mark. Therefore, the PDSI-based drought in the GP is continuous throughout 1988 and 1989. Also, as mentioned in the previous section, the fictitious drought in 2000 in ERA-40 was identified as one of the major disagreements among the NARR, ERA-40, and Dai et al. PDSI results (Fig. 2). Coincidentally, by the objective drought identification criteria used in this exercise, even the NARR would have erroneously indicated a drought in 2000 if relying on soil moisture anomaly alone! One of the unique aspects of PDSI versus any univariate index is that it is intended to monitor drought such that, if the PDSI is negative, a drought *already* exists. If the PDSI remains negative, this means the drought still exists, but is not part of the definition itself. The PDSI does not go negative without just cause; rather, it takes into account a complete picture of the terrestrial water balance and thus has a reasonably good estimate as to whether a drought actually exists versus a month with a deficit of rainfall that could be reversed the following month given rainy conditions. This is in stark contrast to a univariate index (e.g., soil moisture anomaly) where one would need to wait for two more months to establish if a drought is in progress. The implications for monitoring, prediction, and response are obvious.

c. PDSI sensitivity analysis to surface hydrological processes

In this section, we specifically isolate the effects of evaporation, potential evaporation, runoff, and soil moisture on PDSI by subtracting from the regional PDSI indices experimental indices generated by holding one of the processes to climatology. As described in section 2, the PDSI calculation rests on the difference between P and P_{req}, and the aforementioned parameters are relevant to the calculation of P_{req}. Obviously precipitation has a dominant impact on drought, and

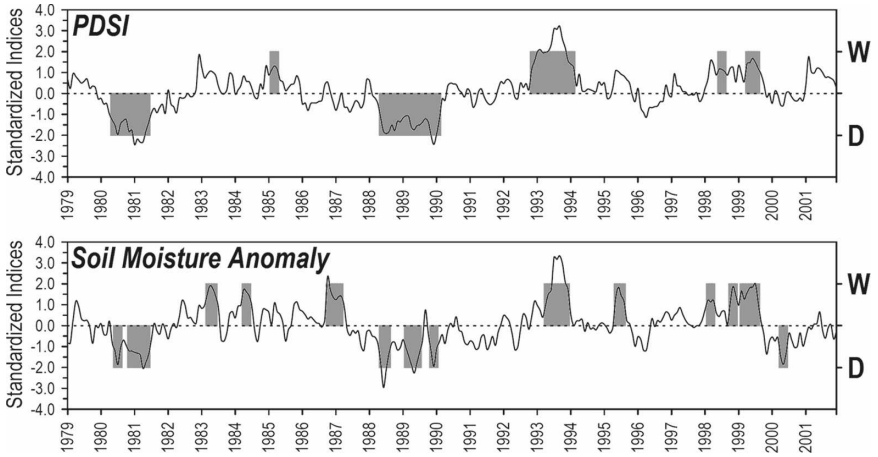

FIG. 6. Normalized monthly time series of (top) PDSI and (bottom) soil moisture anomalies in the GP region from the NARR (thin line) and objectively identified droughts and wet spells (gray shading).

holding precipitation itself to climatology makes little sense: however, we can examine the differences between a temporally smoothed *P* and PDSI, as the other surface hydrological processes must be responsible for the differences. A comparison of precipitation and PDSI, including examination of the scale dependence of these results, is shown in Fig. 7. We define subcontinental scale as the continental United States, regional scale as the GP index region previously defined, and local scale as a single point. The single point chosen for "local" scale (44°N, 93°W) falls over a rural area ~50 miles south of Minneapolis, Minnesota, and is within the domain of the regional scale used (being the GP). On the subcontinental and regional scales (Fig. 7, top and middle), precipitation (temporally smoothed) explains over one-third of the variance of PDSI, and most differences are minor. In contrast, the relative importance of additional surface hydrological processes increases as the spatial scale becomes finer (area over which averages are computed); less than one-third of the PDSI variability is explained by precipitation. Focusing on the severe drought of the late 1980s, at the local scale there is a large difference between the precipitation anomaly and diagnosed PDSI; precipitation was lower than normal but not much more than other dips in the time series, while PDSI indicates a severe and prolonged drought. Thus, on the local scale it seems one or more of those additional surface hydrological processes may have been more important than precipitation itself. With this in mind, the remainder of this section is a discussion of the PDSI results computed with evaporation, potential evaporation, runoff, or soil moisture held to climatology.

The resulting differences are shown in Fig. 8. A positive PDSI difference means the interannual variability of that process resulted in higher PDSI, and vice versa. It should be cautioned, however, that holding a parameter to climatology may lead to some internal inconsistency in hydrological accounting. If, in nature, parameters B and C depend on A, and parameter A is held to climatology, B and C are not adjusted to be consistent with the new specified value of A. Thus, the differences shown are due *strictly* to the parameter in question. To quantify the impact of a parameter on the PDSI, we use the root-mean-square error (RMSE) between the monthly PDSI value in the control output and the output produced by holding that parameter to climatology. The greater the RMSE, the larger impact that parameter's interannual variability has on PDSI evolution. In the NW region (Fig. 8, top), the processes that had the greatest impact on PDSI were evaporation (RMSE = 0.32) and soil moisture (RMSE = 0.39). The fact that soil moisture has a large impact on drought evolution in the western United States is consistent with the findings of Seager et al. (2005), which showed that antecedent soil moisture conditions help determine whether wet or dry conditions in one season will persist into the following season.

In the GP region (Fig. 8, middle), surface hydrological parameters that had the greatest impact on PDSI were evaporation (RMSE = 0.48) and potential evaporation (RMSE = 0.25). Interestingly, soil moisture is not as influential as in the NW region (RMSE = 0.12). The greatly diminished influence of soil moisture on Great Plains PDSI variability must be due to the small amplitude of soil moisture variability in this region: not surprising, given the abundant incoming solar radiation in the summer (i.e., the rainy season in the Great

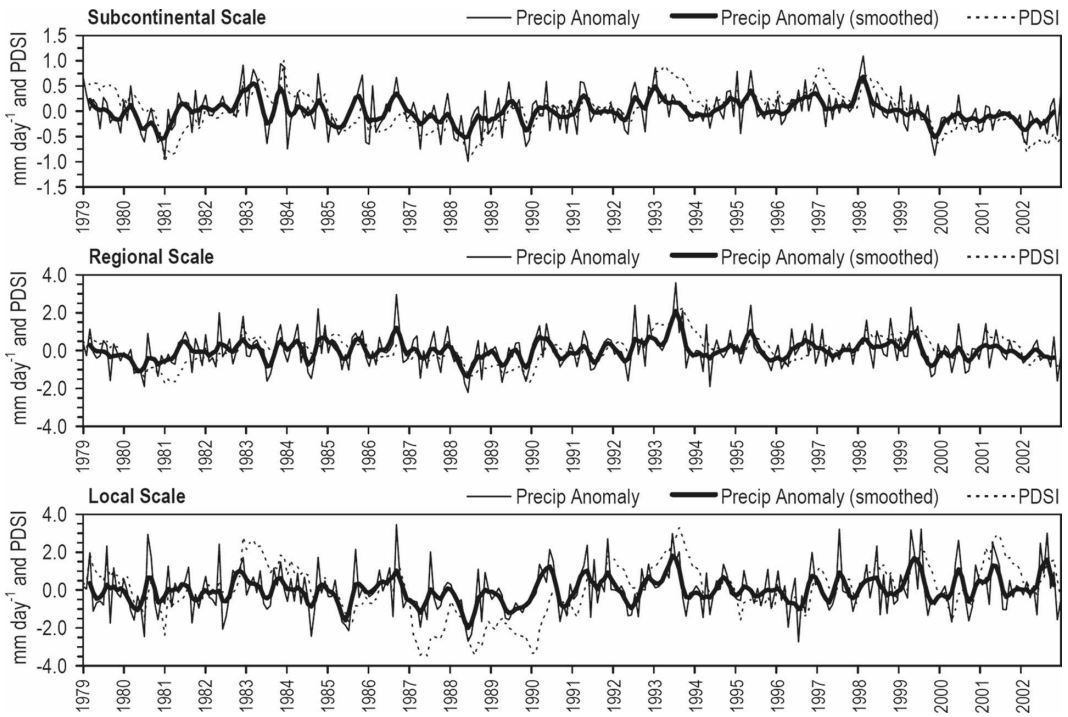

FIG. 7. Time series of precipitation anomaly (thin line), 5-month temporally smoothed precipitation anomaly (heavy line), and PDSI (dashed line) averaged over (top) the United States (subcontinental scale), (middle) GP (regional scale), and (bottom) a single point (44°N, 93°W) within the GP region (local scale). Correlations between the smoothed precipitation anomaly and PDSI are 0.65, 0.59, and 0.55 for subcontinental, regional, and local, respectively.

Plains).[3] The sensitivity to evaporation is understandably stronger since suppression of evaporation variability will lead to large soil moisture anomalies, and thus PDSI variations. In the SE region (Fig. 8, bottom), evaporation (RMSE = 0.34), potential evaporation (RMSE = 0.40), and soil moisture (RMSE = 0.30) had a large impact on PDSI, while runoff (RMSE = 0.14) had the smallest impact.

Focusing on the Great Plains where evaporation had the largest impact on PDSI, the factor by which PDSI is damped or amplified specifically due to evaporation is shown in Fig. 9. In the GP region, the effect of the interannual variations in evaporation is to suppress the interannual variability of drought. Given that the reduced PDSI variability in Fig. 9 is found along the eastern edge of the relative minimum variability in the control results (Fig. 1, bottom left), this is equivalent to an eastward expansion of the region of low PDSI variability into the central GP region. Given the particularly high sensitivity of GP drought conditions to evaporation, careful attention should be paid to how evaporation is treated in further large-scale modeling studies aimed at understanding Great Plains drought variability.

d. Linkages to ocean interannual variability

Given that drought conditions rely heavily upon the cumulative effects of precipitation and temperature, which can be influenced by forcing from remote regions, linkages between North American PDSI variability and large-scale climate variability are addressed in this section. El Niño–Southern Oscillation, the leading mode of interannual ocean–atmosphere variability in the Pacific, strongly influences both regional and distant climates, generating profound teleconnections to both tropical and extratropical regions. An index widely used to mark ENSO variability is the Southern Oscillation index (SOI); the other being the Niño-3.4 sea surface temperature (SST) index. SOI is the difference between sea level pressure anomalies over Tahiti and Darwin, Australia and is linked to sea surface temperature anomalies in the equatorial Pacific Ocean. According to the NOAA/CPC, El Niño conditions (or

[3] Soil moisture *variations* in the Great Plains arise from the imbalance of larger terrestrial water budget terms: precipitation input and the evaporation–runoff fate of regional precipitation, especially in summer.

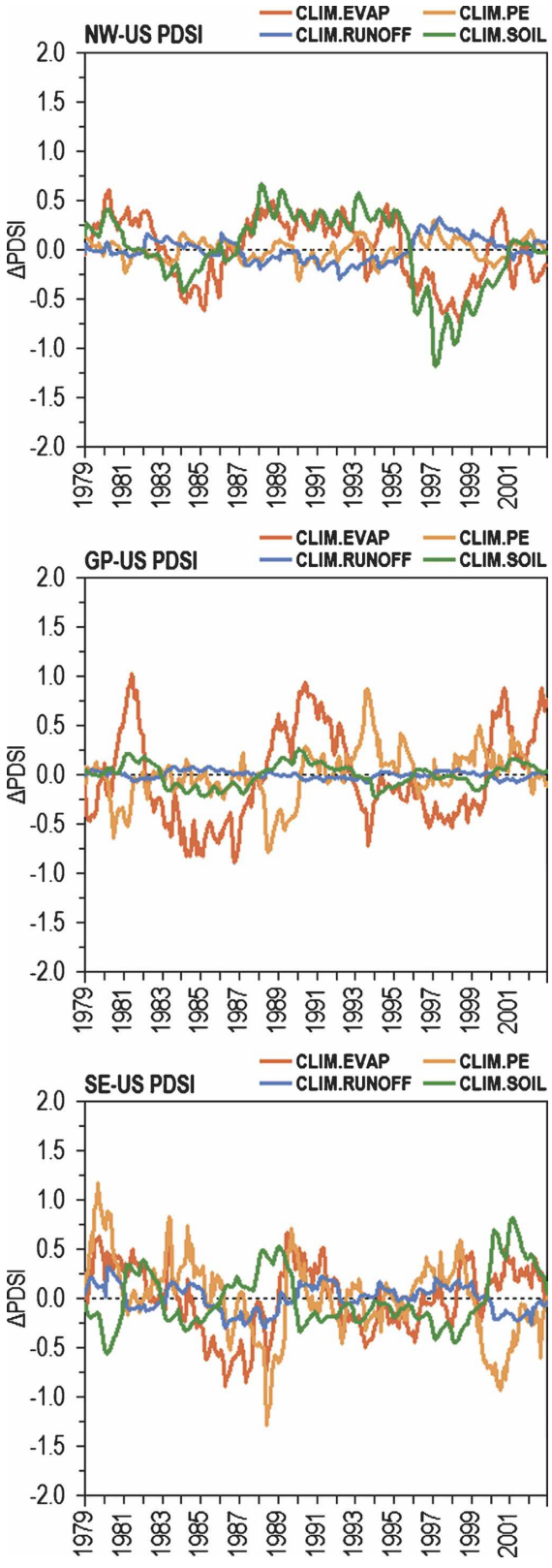

FIG. 8. Time series of monthly NARR PDSI difference (control minus experimental) for climatological evaporation (red), climatological potential evaporation (orange), climatological runoff (blue), and climatological soil moisture (green) in the (top) NW, (middle) GP, and (bottom) SE regions.

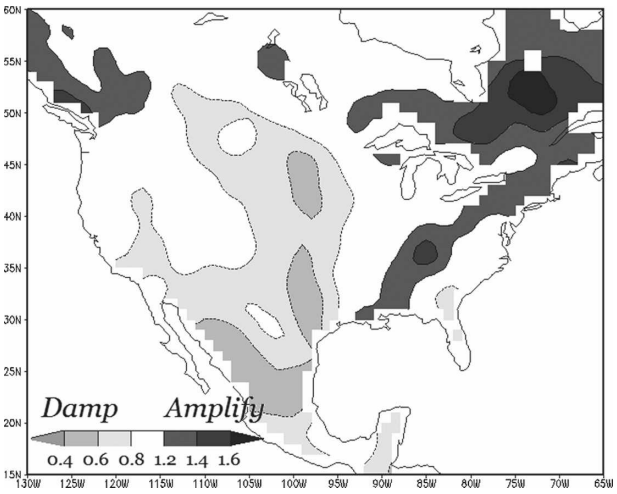

FIG. 9. Ratio of the standard deviation of monthly PDSI (1979–2002) in the control results to those in which climatological evaporation was used. Thus, positive values denote regions where the interannual variability of evaporation results in higher interannual variability of PDSI, and vice versa.

negative SOI) are associated with wet and cool conditions over the Southeast, and the opposite for La Niña events (or positive SOI). In all three datasets, each regional PDSI index is slightly, but significantly, correlated with contemporaneous SOI values. Such correspondence is also evident in the first two PCs of PDSI from NARR and ERA-40. However, as shown by Dai et al. (1998, 2004), Schubert et al. (2004), and Seager et al. (2005), the leading mode of global and North American drought variability is driven by ENSO, and the relationship cannot be summarized simply in terms of contemporaneous correlations.

As shown in a recent modeling study by Seager et al. (2005), the cooling of the eastern equatorial Pacific Ocean, characteristic of La Niña events, sets up an anomalous atmospheric circulation forcing the subtropical jets poleward. The northward-displaced jet in the Northern Hemisphere leads to eddy-driven descent and subsequently reduced precipitation over midlatitude North America. Highly consistent with the precipitation-centric results of Schubert et al. (2004) and Seager et al. (2005), the interannual variability of meteorological drought over the United States in the newly constructed PDSI datasets displays a strong, event-based correspondence with that of equatorial Pacific SSTs. Shown in Fig. 10 is a time–longitude depiction of equatorial Pacific SST anomalies, followed by that of NARR PDSI at three latitude belts across North America, beginning with 35°N ascending in latitude by 5° from left to right. One can clearly see that the 1984 and 1998 La Niñas ("A" and "C" in Fig. 10) were followed by severe U.S. droughts that appear first in the

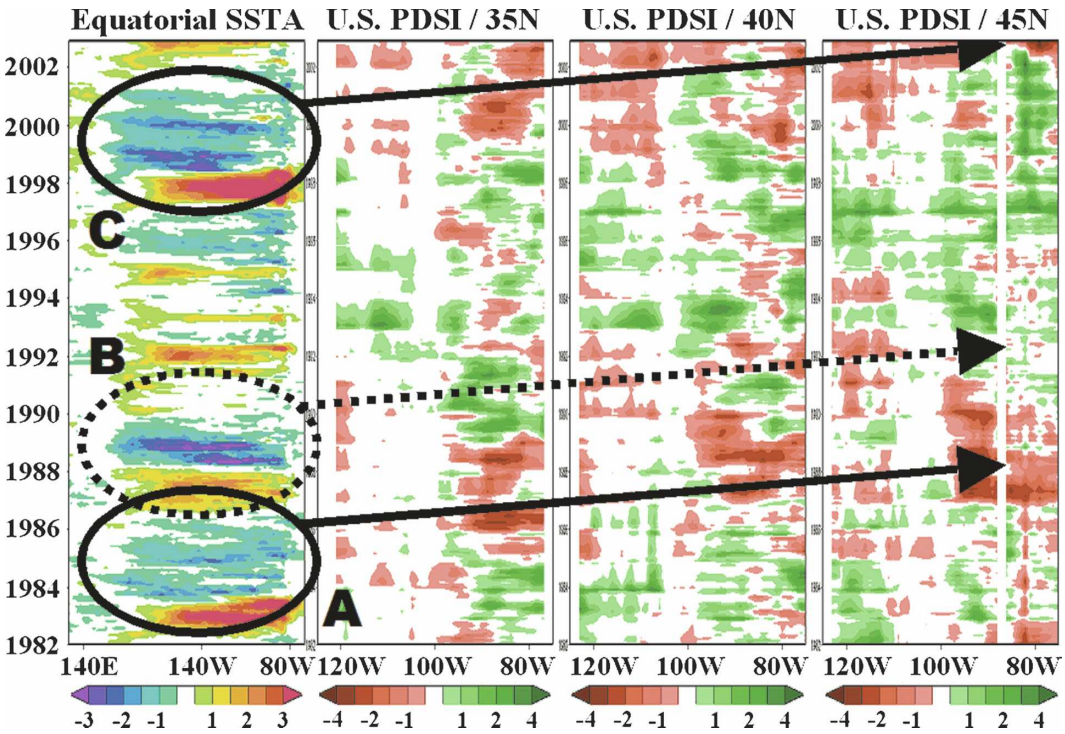

FIG. 10. (from left to right) Time–longitude depictions of the equatorial Pacific SST anomaly (°C) [from Reynolds et al. (2002)] averaged between 2°S and 2°N and the NARR PDSI along 35°N (averaged 33°–37°N), 40°N (averaged 38°–42°N), and 45°N (averaged 43°–47°N). Time increases from January 1982 through December 2002 along the positive direction of the *y* axis. Annotated events are discussed in the main text.

southern latitude belt and propagated northward. Identical time–longitude analyses were also performed on the PDSI dataset derived from ERA-40 dataset, with similar results.

The drought of 1988 has been attributed, among others, to the strong La Niña of 1988 (i.e., "B" in Fig. 10; e.g., Trenberth and Guillemot 1996; Mo et al. 1997). The NARR PDSI evolution displayed in Fig. 10, however, shows that the drought of 1988 actually began in 1986 in the southern latitude belt and propagated through to the northern latitude belt by 1987–88. This can also clearly be seen in the regional PDSI indices in Fig. 2, where the SE PDSI index is leading in this period. While the strong 1988 La Niña may well have prolonged the drought's persistence through the close of the 1980s, it is unlikely to have been involved in the *initiation* of this drought. A similar coevolution of equatorial Pacific SST anomalies and PDSI was set in motion with the 1998 La Niña ("C" in Fig. 10). The drought signals following the 1984 and 1998 La Niña events were quite strong. What the 1984 and 1998 La Niña events have in common is that they were both preceded by a strong El Niño, whereas the 1988 La Niña was only preceded by a moderate El Niño. Similar time–longitude plots of SST anomaly from Kaplan et al. (1998) and PDSI at the 40°N latitude belt from Dai et al. (2004) for the full twentieth century (January 1900–December 1999) are presented in Fig. 11. Kaplan SST anomalies were produced using a combination of EOF projection, optimal interpolation, Kalman filter forecast and analysis, and optimal smoothing (Kaplan et al. 1998). To the extent the Kaplan SST dataset is accurate throughout the twentieth century, one can discern that many U.S. droughts were preceded by La Niñas (e.g., 1910, 1933, 1938, 1955, 1964, 1973–77, and 1989).

To conclude the present section on the influence of interannual SST variations on PDSI, we explore the potential predictability of North American drought from ENSO. At zero lag, there is a significant correlation between the Niño-3.4 index and PDSI over Texas (Fig. 12). This suggests that during El Niño events, which tend to peak in boreal winter, Texas tends to experience wet conditions: during La Niña events Texas tends to experience dry conditions (more accurately, meteorological drought). In the calculation of statistical significance, the number of degrees of freedom was adjusted to account for the decorrelation time scale of ENSO. The Niño-3.4 index has a decorrelation time scale of 5 months, thus the number of degrees of freedom was reduced by a factor of 5 to indicate a

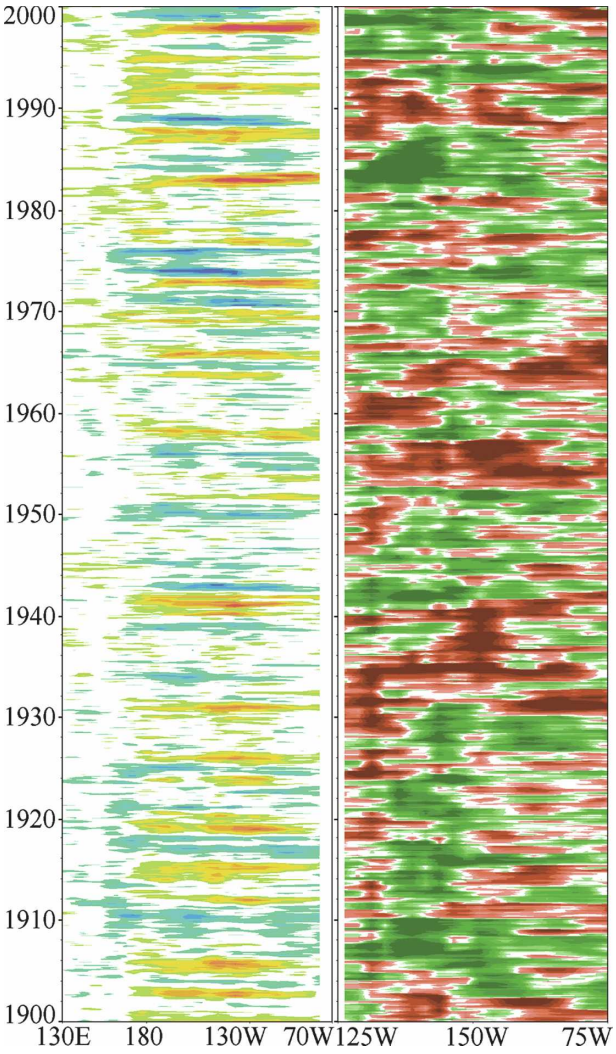

FIG. 11. Time–longitude depictions of (left) the equatorial Pacific SST anomaly (°C) (Kaplan et al. 1998) averaged between 2.5°S and 2.5°N and (right) the Dai et al. (2004) PDSI along 40°N averaged between 38° and 42°N. Time increases from January 1900 through December 1999 along the positive direction of the *y* axis. Color scheme as in Fig. 10.

realistic number of degrees of freedom. At 3-month lag, an ENSO–PDSI connection is apparent over the Southwest, specifically southern California and Arizona, while the signal in the Southeast also strengthens. The picture at 6-month lag is similar, although the correlations over the Southwest and Southeast have peaked and that over Texas begins to diminish. By 9-month lag, the ENSO–PDSI signal persists in the Southwest and Southeast and has all but disappeared over Texas. While apparently the predictability of drought over Texas from ENSO information does not include helpful lead time, there is predictability for drought over the Southwest and Southeast from ENSO information with a lead time of several months. Given that ENSO variance peaks in December–January, the 3-, 6-, and 9-month lags correspond to the beginning, middle, and end of the summertime agricultural season in the United States, respectively. Karl (1983) showed that severe droughts tend to be more persistent in the interior United States, including the Southwest and Texas. Moreover, Karl also found greater springtime predictability in Texas and the Southeast. Our results are highly consistent with Karl (1983), albeit based on a different climate perspective (i.e., remote forcing).

Figure 13 is identical to Fig. 12 except that the PDSI results produced from the ERA-40 are used. The ENSO–PDSI signal displays similar characteristics to the NARR results in the Southeast, with the correlation peaking at 3 and 6 months. The main difference is that the correlation does not appear over southern California and Arizona until the 6-month lag. Finally, to perform a similar analysis with much longer records, in Fig. 14 the PDSI correlations with Niño-3.4 are shown using the Dai et al. PDSI and Kaplan SST dataset over the period 1900–2002. Given the large difference in horizontal resolution of the NARR versus Dai et al. PDSI (1° versus 2.5°), as well as different time periods, one would not expect a perfect match, but the notion that La Niña events tend to correspond with drought conditions over the southern United States in the subsequent spring and summer months holds true when using the longer PDSI and SST datasets. Gaps in the Dai et al. PDSI dataset during the twentieth century prevent analysis over much of the Southwest and the deep Southeast, however, the positive values found over northern Florida and Georgia at 3- and 6-month lag makes it tempting to guess that there would be some continuity (and thus even more similarity with the shorter NARR results) along the deep Southeast adjacent to the Gulf of Mexico, if the resolution and coverage of the dataset would have allowed it.

In keeping with the Palmer perspective on meteorological drought (i.e., the hydroclimate context is set by temperature and precipitation), it is of interest to know whether the ENSO–PDSI connection over the southern United States is due to ENSO remotely forcing anomalies of surface air temperature, precipitation, or both. Dai et al. (2004) surmised that ENSO-related precipitation patterns were primarily responsible for the connection between tropical Pacific SSTs and PDSI, while surface air temperature played a negligible role in that teleconnection. Although a shorter record than Dai et al. (2004), higher resolution and more sophisticated datasets such as the NARR prompt revisiting this question.

Beginning with the contemporaneous correlation between PDSI over Texas and ENSO, Figs. 15a and 15c

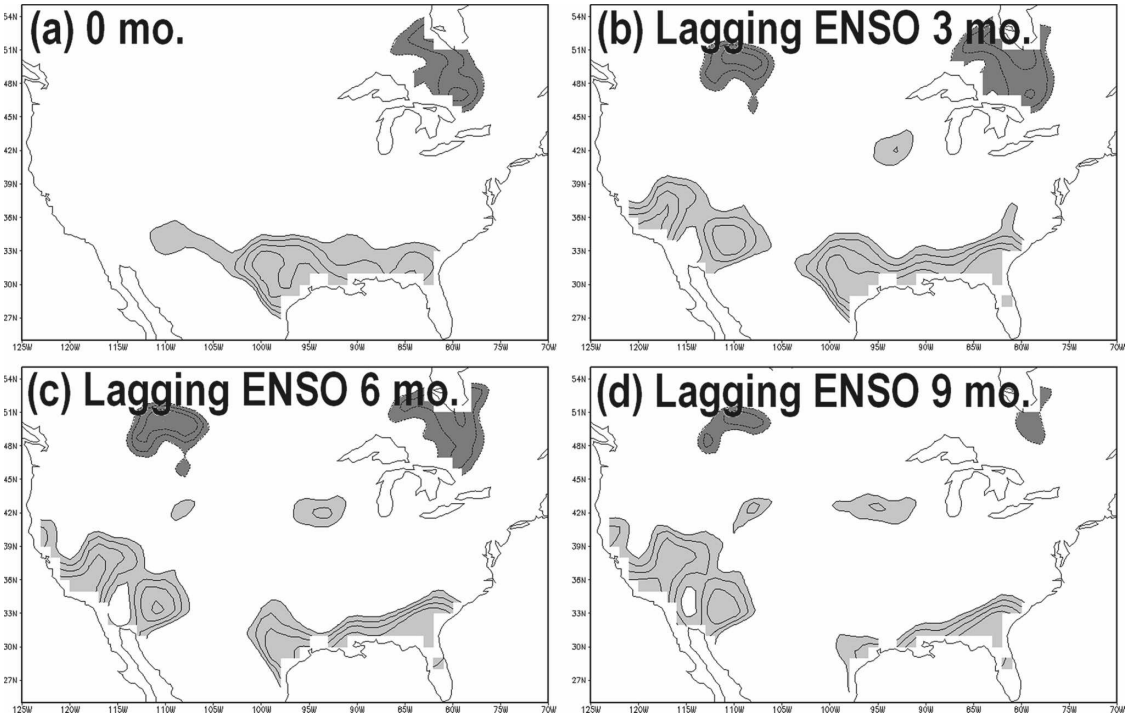

FIG. 12. Maps of the correlation between NARR PDSI and the Niño-3.4 index at (a) 0 lag, (b) 3-month lag, (c) 6-month lag, and (d) 9-month lag for the period 1979–2002. Only values significant at the 95% confidence level are shown; contour interval is 0.05.

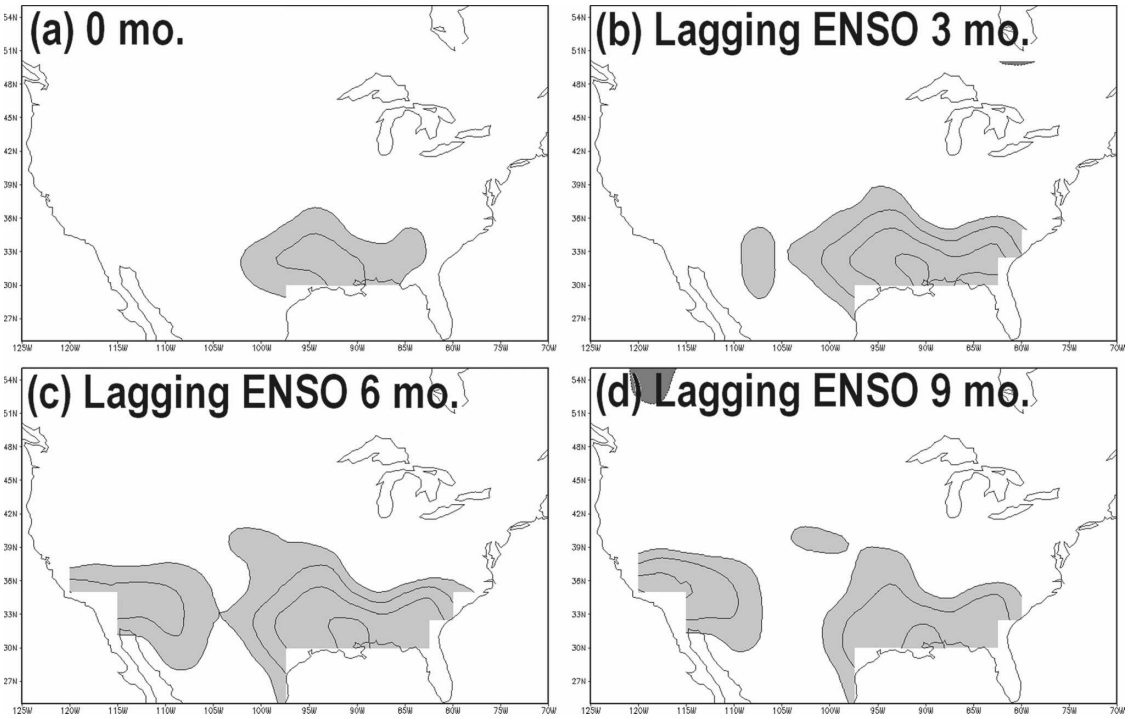

FIG. 13. As in Fig. 12 but of the correlation between ERA-40 PDSI and the Niño-3.4 index.

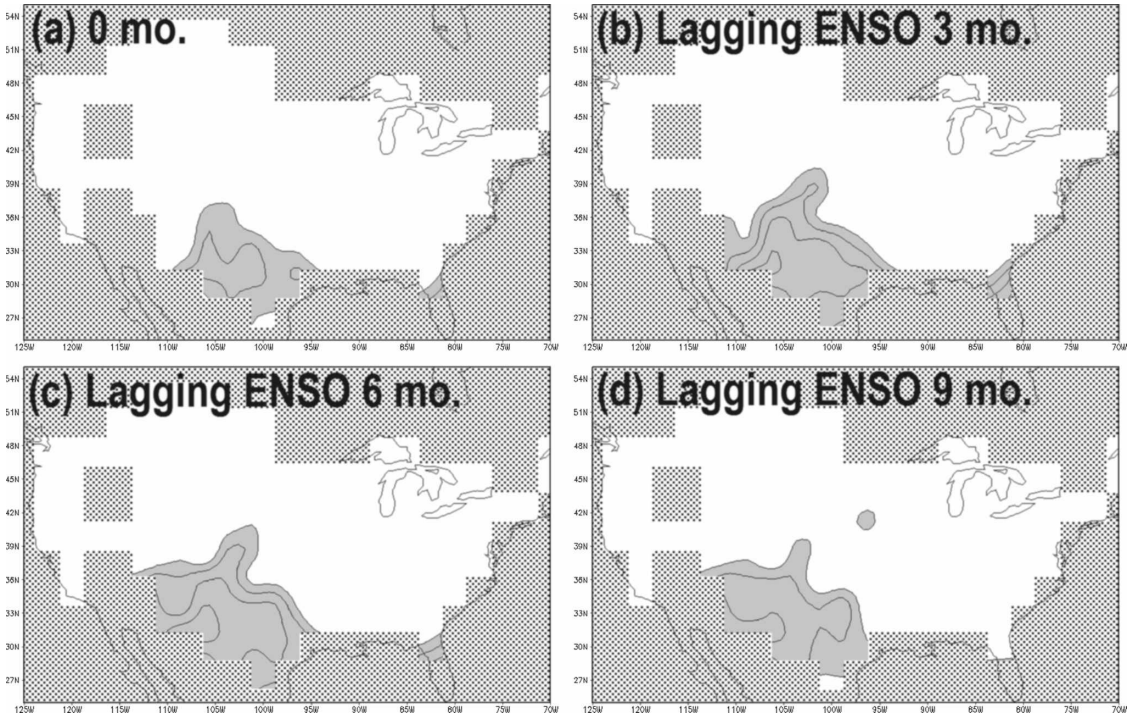

FIG. 14. As in Fig. 12 but of the correlation between the Dai et al. PDSI and the Niño-3.4 index for the period 1900–2003. Gray shading indicates regions where there is insufficient data in the Dai et al. PDSI dataset.

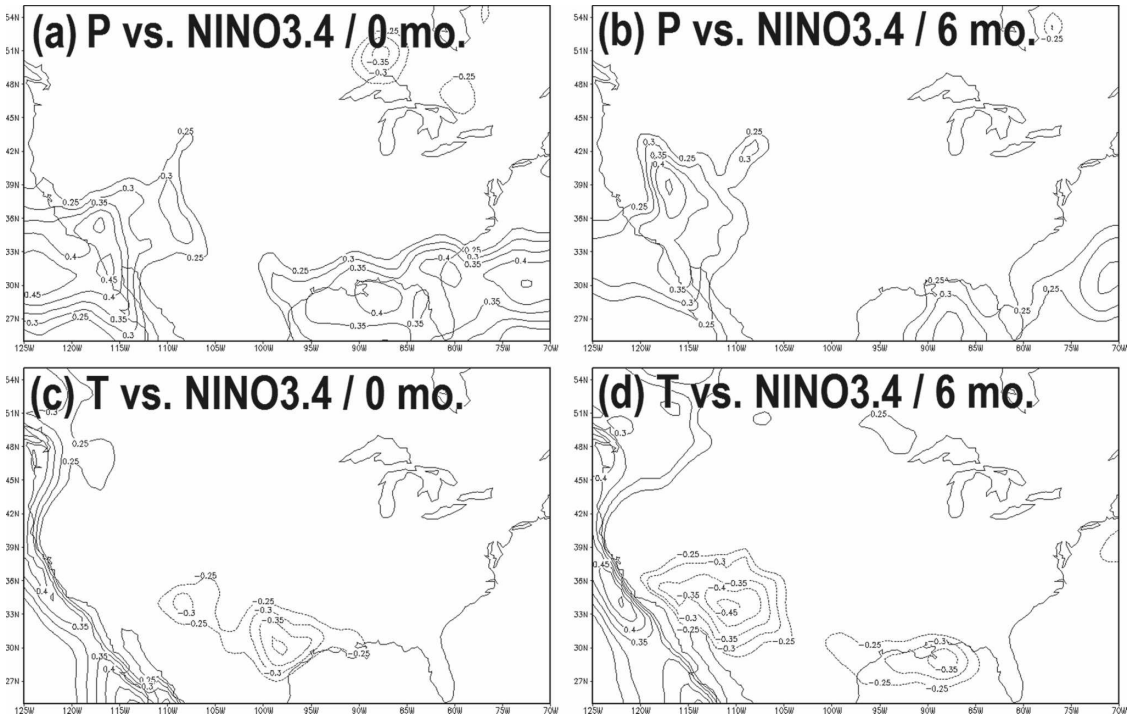

FIG. 15. Maps of the correlation between 5-month smoothed NARR precipitation and the Niño-3.4 index at (a) 0 lag and (b) 6-month lag and the correlation between 5-month smoothed surface air temperature at (c) 0 lag and (d) 6-month lag for the period 1979–2002. Only values significant at the 95% confidence level are shown; contour interval is 0.05.

suggest that, for example, La Niña events force warm surface air temperature anomalies over Texas, closely resembling the pattern of the PDSI correlation with ENSO (i.e., Fig. 12a), as well as negative precipitation anomalies over a broad region covering the northern Gulf of Mexico and adjacent coastal states. Such a configuration helps explain why Texas experiences wet (dry) conditions during El Niño (La Niña) events at zero lag, while the other coastal states do not. This is yet another example of why precipitation alone cannot be used as an indicator of drought; at zero lag precipitation is correlated with ENSO over the Southwest and Southeast, but without the temperature anomaly drought does not develop there. Moving to the 6-month lag, the surface air temperature and precipitation anomalies have diminished over Texas (as did the PDSI correlation; Fig. 12c). In the Southwest at 6-month lag, positive correlations with precipitation and negative correlations with surface air temperature develop. Clearly both precipitation and temperature are important factors in the method of communication between ENSO and drought over the Southwest. Over the Southeast at 6-month lag, the surface air temperature anomaly is still correlated with ENSO, while the signal in precipitation has moved southward and is not correlated with ENSO over land areas adjacent to the Gulf of Mexico. Again it appears as though surface air temperature is doing a surprising amount of legwork in communicating ENSO's influence on drought conditions by way of modulating evaporation.

e. The North American drought of 1988

The drought of 1988 was the most severe in U.S. history since the Dust Bowl of the 1930s. The economic loss due to crop damages alone is estimated to be $40 billion (Kogan 1997). In this section we compare the representations of the drought of 1988 by the PDSI datasets derived from the NARR, ERA-40, and that of Dai et al. (2004) and the NOAA/CPC operational product. The height of the drought, according to PDSI maps issued by NOAA/CPC, was July 1988. Thus, the July 1988 PDSI from all four datasets are shown in Fig. 16. By July 1988, the upper Midwest extending nearly to the West coast was in a state of severe state of drought with moderate-to-severe drought conditions prevailing also in the SE region. The PDSI diagnosed from NARR underestimates the severity of the drought in the upper Midwest west of the Dakotas, while the ERA-40-based index underestimates drought in the SE region. In this case, the drought representation produced by Dai et al. (2004) is in excellent agreement with the NOAA/CPC product, including the wet conditions in Arizona and New Mexico.

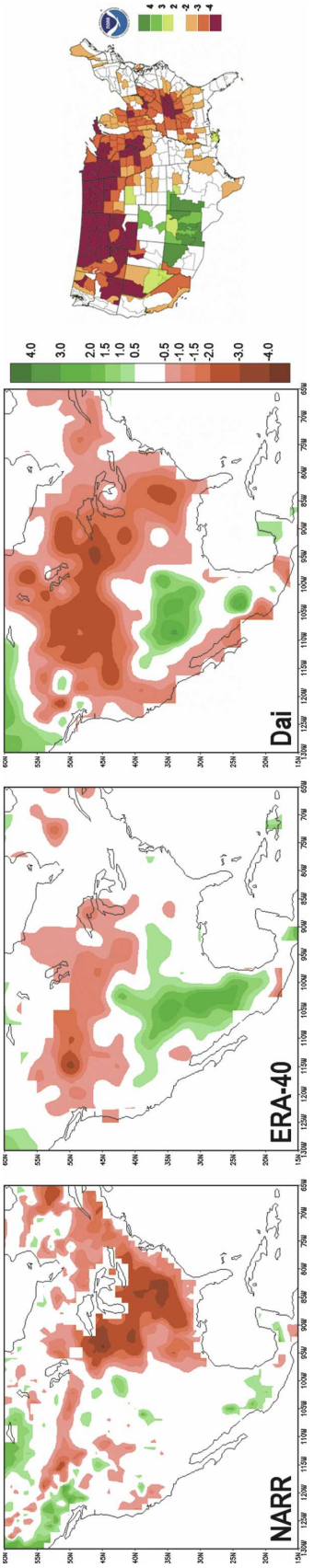

FIG. 16. PDSI maps from NARR, ERA-40, Dai et al. (2004), and the NOAA operational product for July 1988.

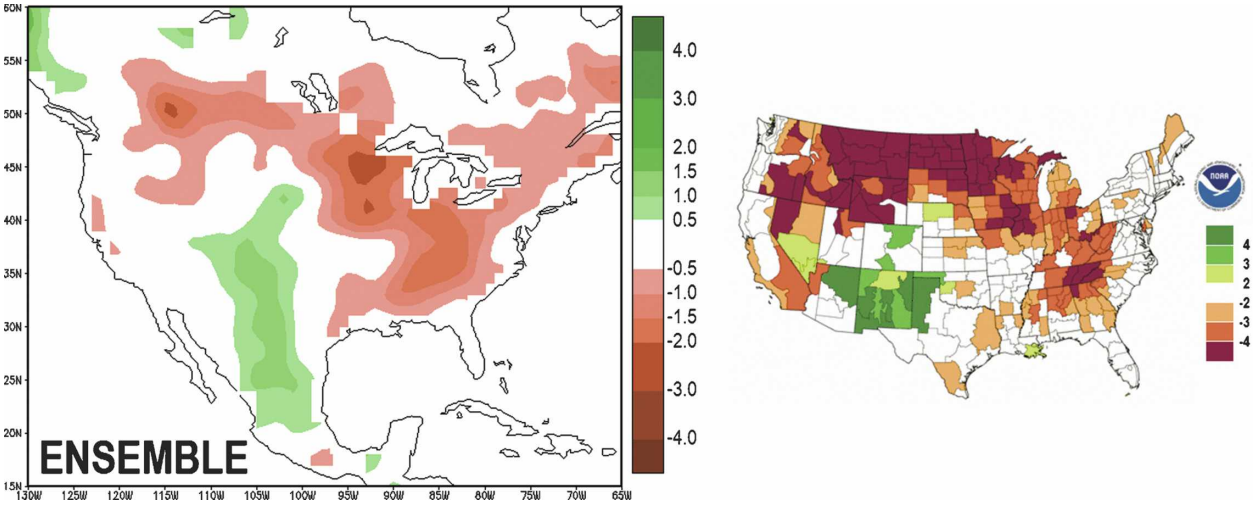

FIG. 17. PDSI maps for the (left) NARR–ERA-40 ensemble and (right) NOAA operational product for July 1988.

As the drought intercomparison shown in Fig. 16 is only for a single month, we note the neighboring month differences between the NARR, ERA-40, and the Dai et al. regional PDSI indices from Fig. 2. In the NW time series (Fig. 2, top), the drought conditions in the NW were clearly underestimated by both NARR and ERA-40 as compared to Dai et al. In the GP time series (Fig. 2, middle), there is good agreement between all three sources with the exception of a late initiation in ERA-40. In the SE time series (Fig. 2, bottom), severe drought conditions from 1987 to 1988 are all but missed in ERA-40, while there is excellent agreement between the NARR and Dai et al. PDSI results.

Given that the NARR estimate of the drought picture in July 1988 sufficiently represented the drought in the SE region and underestimated the drought in the northern United States, while the ERA-40 estimate was the opposite, one might wonder what an ensemble combining the PDSI estimates from NARR and ERA-40 would depict. Figure 17 presents the "ensemble" mean PDSI map alongside the NOAA operational product for July 1988. The ensemble was constructed by regridding the native 2.5° ERA-40 PDSI map to 1°, taking the arithmetic mean with the native 1° NARR PDSI map, and applying a nine-point spatial smoother. The spatial distribution of drought and wet conditions in the United States is much improved, drawing on the apparent strengths of either estimate.

Returning to the sensitivity style experimental results discussed in the previous section, in Fig. 18 the July 1988 NARR PDSI results for each of the experimental scenarios are shown. As noted in section 3c, the processes having the greatest impact on PDSI in the NW region were evaporation and soil moisture. Evident in both the evaporation and soil moisture experimental PDSI results (Fig. 18, second and fifth panels, respectively), drought conditions in the upper Midwest and NW would have had a different representation in July 1988 given suppressed interannual variability of such processes, especially evaporation. Thus, using PDSI as a sort of model diagnostic, it is apparent that evaporation was too weak in the summer of 1988 in the NARR.

f. Other notable cases

Based on the time series of PDSI from the three U.S. index regions (Fig. 2), four additional cases were chosen for intercomparison using the two newly constructed PDSI datasets, the Dai et al. PDSI dataset, and operational PDSI maps issued by the NOAA/CPC. Cases were chosen primarily to represent a diversity of regional conditions. The months chosen for intercomparison were April 1981 when drought conditions were indicated for GP and SE; July of 1986 when the SE was under severe drought; July 1989 when neutral conditions were indicated in NW, drought conditions in GP, and wet conditions in SE; and May 1992 when drought conditions were indicated in NW. The intercomparisons for these four cases are shown row-by-row in Fig. 19.

The drought depictions of NARR, ERA-40, Dai et al., and NOAA for April 1981 are shown in Fig. 19 (top). NOAA indicates broad and severe drought conditions throughout the U.S. Great Plains and southeastern regions with particularly severe drought in the mid-Atlantic states, eastern Texas, Missouri, and the upper Midwest. The spatial pattern of PDSI in April 1981 is very close to a physical realization of the NARR

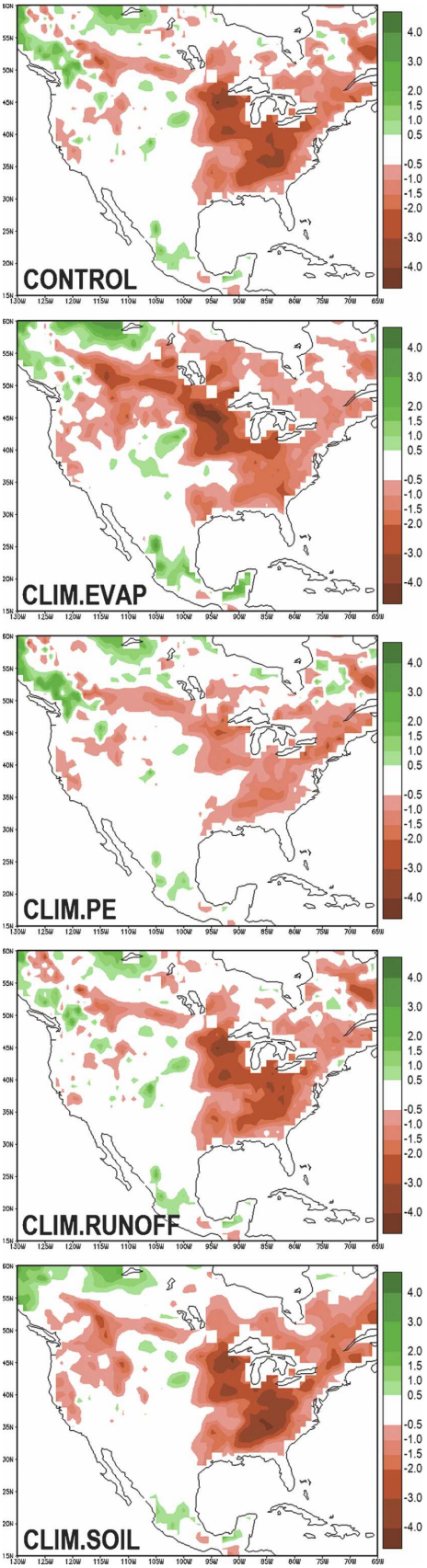

EOF1–ERA-40 EOF2 pair (Fig. 4), which is indeed a recurrent and persistent pattern in the United States. The NARR results capture well the severe conditions in the mid-Atlantic states, eastern Texas, and Missouri, but underestimate the drought conditions in the upper Midwest. The ERA-40 PDSI shows symmetric results well capturing the conditions in the upper Midwest, but underestimating the drought in the mid-Atlantic states. The Dai PDSI agrees well with the NOAA product.

Presented in the second row in Fig. 19 are the drought depictions for July 1986. This period was characterized by a severe drought over the Southeast and the mid-Atlantic states, moderate drought conditions in Wyoming, and scattered wet conditions elsewhere in the United States. The NARR PDSI results represent accurately the structure and severity of the SE drought, while missing the moderate drought in Wyoming. As was the case in April 1981, the ERA-40 drought depiction is symmetric; underestimating the SE drought but overestimating drought conditions in the western Great Plains and NW. While the NARR most accurately represented the structure and severity of the SE drought, Dai et al. have the best overall continental-scale structure.

Figure 19 (third) shows drought maps for July 1989. The NOAA product indicates that there were widespread wet conditions stretching from eastern Texas along the Gulf Coast northward into New England. At the same time, the upper Midwest was experiencing severe drought conditions. The Dai et al. index captures the continental-scale structure again quite accurately. The NARR captures the rapid transition between the Southeast and central U.S. regions well, but does not indicate drought conditions farther to the west, that is, in the very region where PDSI variability was anemic (Fig. 1, bottom-left panel) and EOF loadings minimal (Fig. 4, top). The ERA-40 PDSI results would be considered poor by any metric, with the exception of slight drought conditions over the GP region.

The final case selected was May 1992 (Fig. 19, bottom) when the Southwest was extremely wet and the northwest severely dry. From the maps and the NW PDSI time series (Fig. 2), it is apparent that all three datasets depicted drought conditions in the NW region with ERA-40 being the most severe. The ERA-40 results are in better agreement with the NOAA product

←

FIG. 18. PDSI maps from NARR control and experimental results for July 1988: (from top to bottom) Control (interannually varying everything), climatological evaporation, climatological potential evaporation, climatological runoff, and climatological soil moisture.

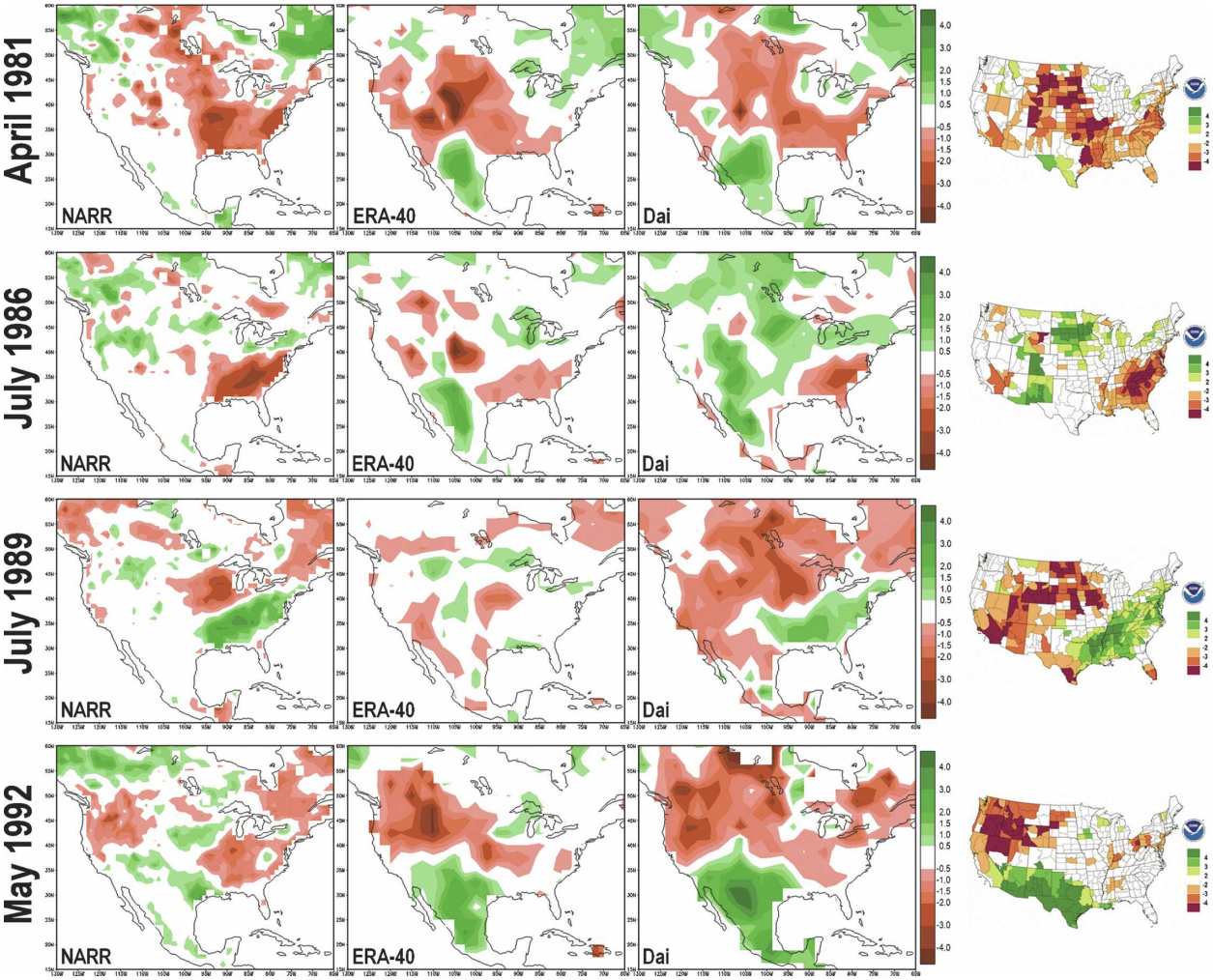

FIG. 19. PDSI maps from NARR, ERA-40, Dai et al. (2004), and the NOAA operational product (from top to bottom) for April 1981, July 1986, July 1989, and May 1992.

than the NARR, as the NARR results are systematically plagued by a lack of variability over the band stretching from Mexico to the Canadian border between about 105° and 100°W. The structure and severity of the wet and dry centers are quite similar between the coarser ERA-40 and Dai et al. PDSI maps, with the Dai et al. indicating the drought center in the NW closer to that of the NOAA product.

4. Summary

In this paper, we construct PDSI datasets consistent with the NARR and ERA-40. The original Palmer (1965) formulation of the PDSI requires only precipitation and temperature to infer a great deal of information about the state of the surface hydrological budget and how the soil will respond on a local basis. However, our approach is unique in that we attempt to exploit input and intermediate variables provided directly by reanalyses, rather than relying on rudimentary calculations for each term in the water balance. The resulting PDSI datasets from the NARR and ERA-40 show promise for use in understanding North American drought variability, including some reasonably accurate (w.r.t. the NOAA operational PDSI product) representations of drought conditions across the United States over the past two decades. This methodology can be used with other suitable reanalyses and applied to problems abroad. For example, while preparing the present manuscript, Australia is experiencing its worst drought in perhaps 1000 yr, with back-to-back summers of failed crops spread over eastern Australia, and the government is considering a ban on irrigation in the country's primary agricultural area. At the same time,

the Australian Commonwealth Scientific and Industrial Research Organization (CSIRO) is completing the second phase of the Australian Water Availability Project (AWAP), which is similar to the NARR in that it combines observational data and models to provide the best current and retrospective analysis of the state of Australia's terrestrial water balance (Raupach et al. 2007). Since the AWAP will provide a retrospective analysis from 1900 to present, new insight into the interannual-to-interdecadal variations of Australian drought may be generated by applying the methodology described in this paper to the AWAP.

Evaporation was shown to be an important process in the representation of drought conditions through comparison with parallel calculations wherein that process was held to its climatological value. This was especially true in the Great Plains and eastern United States, which highlights the need for improved and sustained measurements of evaporations and the environmental controls on evaporation in these regions for monitoring drought.

The comparison with ocean interannual variability confirms the considerable influence of ENSO on the temporal variations of drought conditions over the United States. This is consistent with previous work explaining mechanistic links between North American drought variability and major patterns based in the tropical Pacific. The prospect of drought forecasts with lead times of multiple seasons aided by an understanding of tropical oceanic influences is encouraging, but it is important to quantify the strengths and limitations associated with regional and global reanalyses of cumulative drought conditions. We feel that the PDSI is one appropriate metric, in part because the observational and operational benchmarks exist, but also because the PDSI is already within the lexicon of agricultural and water management sectors. The PDSI datasets produced in this study, as well as PSDI source codes, are freely available upon request.

Acknowledgments. The authors gratefully acknowledge Dr. Aiguo Dai for kindly lending his PDSI code to be used as a point of reference. We also thank three anonymous reviewers for helpful comments and suggestions. Historical PDSI maps were downloaded from the NOAA National Climatic Data Center (NCDC) Web site (http://lwf.ncdc.noaa.gov/oa/climate/research/drought/palmer-maps/). The Dai PDSI dataset, Reynolds et al. (OI v2) SST dataset, and Kaplan SST v2 datasets were provided by the NOAA/OAR/ESRL PSD, Boulder, Colorado, from their Web site (http://www.cdc.noaa.gov/PublicData/).

REFERENCES

Alley, W. M., 1984: The Palmer Drought Severity Index: Limitations and assumptions. *J. Climate Appl. Meteor.,* **23,** 1100–1109.

Barlow, M., S. Nigam, and E. H. Berbery, 2001: ENSO, Pacific decadal variability, and U.S. summertime precipitation, drought, and streamflow. *J. Climate,* **14,** 2105–2128.

Black, T. L., 1994: The new NMC mesoscale eta model: Description and forecast samples. *Wea. Forecasting,* **9,** 265–278.

Budyko, M. I., 1958: *The Heat Balance of the Earth's Surface.* U.S. Department of Commerce, 259 pp. (Translated from Russian by N. A. Stepanova.)

Chen, M., P. Xie, J. E. Janowiak, and P. A. Arkin, 2002: Global land precipitation: A 50-yr monthly analysis based on gauge observations. *J. Hydrometeor.,* **3,** 249–266.

Dai, A., K. E. Trenberth, and T. Karl, 1998: Global variations in droughts and wet spells: 1900-1995. *Geophys. Res. Lett.,* **25,** 3367–3370.

——, ——, and T. Qian, 2004: A global dataset of Palmer Drought Severity Index for 1870–2002: Relationship with soil moisture and effects of surface warming. *J. Hydrometeor.,* **5,** 1117–1130.

Ek, M. B., K. E. Mitchell, Y. Lin, E. Rogers, P. Grunmann, V. Koren, G. Gayno, and J. D. Tarpley, 2003: Implementation of Noah land surface model advances in the National Centers for Environmental Prediction operational mesoscale Eta model. *J. Geophys. Res.,* **108,** 8851, doi:10.1029/2002JD003296.

Fan, Y., H. M. Van den Dool, D. Lohmann, and K. Mitchell, 2006: 1948–98 U.S. hydrological reanalysis by the Noah land data assimilation system. *J. Climate,* **19,** 1214–1237.

Ghil, M., and Coauthors, 2002: Advanced spectral methods for climatic time series. *Rev. Geophys.,* **40,** 1003, doi:10.1029/2000RG000092.

Heim, R. R., Jr., 2002: A review of twentieth-century drought indices used in the United States. *Bull. Amer. Meteor. Soc.,* **83,** 1149–1165.

Jones, P. D., and A. Moberg, 2003: Hemispheric and large-scale surface air temperature variations: An extensive revision and an update to 2001. *J. Climate,* **16,** 206–223.

Kalnay, E., and Coauthors, 1996: The NCEP/NCAR 40-Year Reanalysis Project. *Bull. Amer. Meteor. Soc.,* **77,** 437–471.

Kaplan, A., M. Cane, Y. Kushnir, A. Clement, M. Blumenthal, and B. Rajagopalan, 1998: Analyses of global sea surface temperature 1856-1991. *J. Geophys. Res.,* **103,** 18 567–18 589.

Karl, T. R., 1983: Some spatial characteristics of drought duration in the United States. *J. Climate Appl. Meteor.,* **22,** 1356–1366.

——, 1986: The sensitivity of the Palmer Drought Severity Index and Palmer's Z-Index to their calibration coefficients including potential evaporation. *J. Climate Appl. Meteor.,* **25,** 77–86.

Kogan, F., 1997: Global drought watch from space. *Bull. Amer. Meteor. Soc.,* **78,** 621–636.

Mesinger, F. G., and Coauthors, 2004: NCEP North American Regional Reanalysis. Preprints, *15th Symp. on Global Change and Climate Variations,* Seattle, WA, Amer. Meteor. Soc., P1.1. [Available online at http://ams.confex.com/ams/pdfpapers/72502.pdf.]

Mo, K. C., and M. Chelliah, 2006: The modified Palmer Drought Severity Index based on the NCEP North American Regional Reanalysis. *J. Appl. Meteor. Climatol.,* **45,** 1362–1375.

——, J. Nogues Paegle, and R. Wayne Higgins, 1997: Atmospheric processes associated with summer floods and

droughts in the central United States. *J. Climate,* **10,** 3028–3046.

Nigam, S., and A. Ruiz-Barradas, 2006: Seasonal hydroclimate variability over North America in global and regional reanalyses and AMIP Simulations: A mixed assessment. *J. Climate,* **19,** 815–837.

——, M. Barlow, and E. H. Berbery, 1999: Analysis links Pacific decadal variability to drought and streamflow in United States. *Eos, Trans. Amer. Geophys. Union,* **80,** 621, 622, 625.

Palmer, W. C., 1965: Meteorological drought. U.S. Weather Bureau Research Paper 45, 58 pp.

——, and A. V. Havens, 1958: A graphical technique for determining evapotranspiration by the Thornthwaite method. *Mon. Wea. Rev.,* **86,** 123–128.

Penman, H. L., 1948: Natural evaporation from open water, bare soil, and grass. *Proc. Roy. Soc. London,* **193A,** 120–146.

Raupach, M. R., P. R. Briggs, E. A. King, M. Paget, and C. M. Trudinger, 2007: Australian Water Availability Project (AWAP) CSIRO Marine and Atmospheric Research Component. Final Rep. for Phase 2, 38 pp.

Reynolds, R. W., N. A. Rayner, T. M. Smith, D. C. Stokes, and W. Wang, 2002: An improved in situ and satellite SST analysis for climate. *J. Climate,* **15,** 1609–1625.

Ruiz-Barradas, A., and S. Nigam, 2006: Great Plains hydroclimate variability: The view from North American Regional Reanalysis. *J. Climate,* **19,** 3004–3010.

Schubert, S. D., M. J. Suarez, P. J. Pegion, R. D. Koster, and J. T. Bacmeister, 2004: Causes of long term drought in the U.S. Great Plains. *J. Climate,* **17,** 485–503.

Seager, R., Y. Kushnir, C. Herweijer, N. Naik, and J. Velez, 2005: Modeling of tropical forcing of persistent droughts and pluvials over western North America: 1856–2000. *J. Climate,* **18,** 4068–4091.

Sellers, W. D., 1964: Potential evapotranspiration in arid regions. *J. Appl. Meteor.,* **3,** 98–104.

Shafran, P., J. Woollen, W. Ebisuzaki, W. Shi, Y. Fan, R. Grumbine, and M. Fennessy, 2005: Observational data used for assimilation in the NCEP North American Regional Reanalysis. Preprints, *14th Conf. on Applied Climatology,* San Diego, CA, Amer. Meteor. Soc., 1.4. [Available online at http://ams.confex.com/ams/pdfpapers/71689.pdf.]

Thornwaite, C. W., 1948: An approach toward a rational classification of climate. *Geogr. Rev.,* **38,** 55–94.

Trenberth, K. E., and C. J. Guillemot, 1996: Physical processes involved in the 1988 drought and 1993 floods in North America. *J. Climate,* **9,** 1288–1298.

Uppala, S. M., and Coauthors, 2005: The ERA-40 Re-Analysis. *Quart. J. Roy. Meteor. Soc.,* **131,** 2961–3012.

Webb, R. S., C. E. Rosenzweig, and E. R. Levine, 1993: Specifying land surface characteristics in general circulation models: Soil profile data set and derived water holding capacities. *Global Biogeochem. Cycles,* **7,** 97–108.